Anion–π Catalysis of Enolate Chemistry: Rigidified Leonard Turns as a General Motif to Run Reactions on Aromatic Surfaces

Yoann Cotelle[+], Sebastian Benz[+], Alyssa-Jennifer Avestro, Thomas R. Ward, Naomi Sakai, and Stefan Matile*

Abstract: *To integrate anion–π, cation–π, and ion pair–π interactions in catalysis, the fundamental challenge is to run reactions reliably on aromatic surfaces. Addressing a specific question concerning enolate addition to nitroolefins, this study elaborates on Leonard turns to tackle this problem in a general manner. Increasingly refined turns are constructed to position malonate half thioesters as close as possible on π-acidic surfaces. The resulting preorganization of reactive intermediates is shown to support the disfavored addition to enolate acceptors to an absolutely unexpected extent. This decisive impact on anion–π catalysis increases with the rigidity of the turns. The new, rigidified Leonard turns are most effective with weak anion–π interactions, whereas stronger interactions do not require such ideal substrate positioning to operate well. The stunning simplicity of the motif and its surprisingly strong relevance for function should render the introduced approach generally useful.*

"*R*ien ne sert de courir; il faut partir à point. Le Lièvre et la Tortue en sont un témoignage." Thus begins Jean de La Fontaine (1621–1695 AD) to recount the ancient Greek fable from Aesop (620–560 BC). The result is known. In the context of chemical transformations, Aesop's fable perfectly describes the challenge to selectively catalyze a disfavored reaction. A most intriguing example for "tortoise-and-hare catalysis" occurs at the beginning of the biosynthesis of most natural products and is repeated most impressively in the polyketide pathway.[1] Malonyl-CoA, a malonic acid half thioester (MAHT), has evolved as the substrate of choice to accom-

plish the involved enolate chemistry under biological conditions. However, under unoptimized conditions without enzymes in solution, the addition of MAHTs, such as **1a**, via malonate half thioester (MHT) conjugate bases, to enolate acceptors, such as nitroolefin **2**, fails to cleanly generate the relevant addition product **3a** (Figure 1).[2] Instead, decarboxylation is the favored reaction, leading to the less useful thioester **4a** as the major product. Several elegant solutions have been developed to tame the capricious MHT anions, including bioinspired approaches to asymmetric enolate addition to various acceptors.[3]
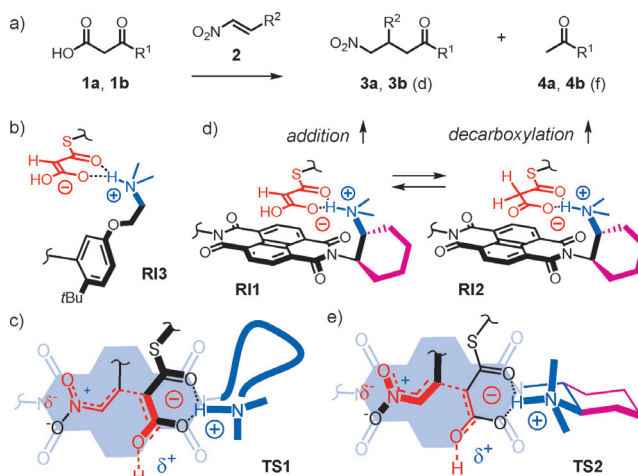

Figure 1. a) Addition of MAHT **1a** (R^1 = SPMP, PMP = *para*-methoxyphenyl) or β-keto acid **1b** (R^1 = Ph) to nitroolefin **2** (R^2 = Ph), forming the disfavored (d) addition products **3a/3b** or the favored (f) decarboxylation products **4a/4b**. b) The original *meta*-aryl turns place the enolate tautomer far from the π surface. c) "Top-down" addition of remote enolates (**RI3**) to nitroolefins on the π surface. d) Fixed (magenta) Leonard turns should place MHTs close to the π surface to influence the equilibrium between the MHT tautomers. e) "Bottom-up" addition of enolates on the π surface (**RI1**) to nitroolefins far from the π surface.

Complementary to the more common cation–π interactions on π-basic aromatic surfaces,[4] anion–π interactions occur on π-acidic surfaces. Their existence has been proposed by theoreticians a bit more than a decade ago and verified experimentally for the solid, solution, and gas phase.[5,6] The functional relevance of anion–π interactions has been demonstrated for self-assembly,[7] transport,[8,9] and, most recently, also for catalysis.[2,10,11] In this context, the selective acceleration of the disfavored addition of MAHT **1a** to nitro-

[*] Dr. Y. Cotelle,[+] S. Benz,[+] Dr. A.-J. Avestro, Dr. N. Sakai, Prof. S. Matile
Department of Organic Chemistry
National Centre of Competence in Research (NCCR) Molecular Systems Engineering
University of Geneva, Geneva (Switzerland)
E-mail: stefan.matile@unige.ch
Homepage: www.unige.ch/sciences/chiorg/matile/

Dr. A.-J. Avestro
Department of Chemistry, Northwestern University
Evanston IL (USA)

Dr. A.-J. Avestro
Current address: Department of Chemistry
University of Durham, Durham (UK)

Prof. T. R. Ward
Department of Chemistry
NCCR Molecular Systems Engineering
University of Basel, Basel (Switzerland)

[+] These authors contributed equally to this work.

Supporting information for this article can be found under http://dx.doi.org/10.1002/anie.201600831.

olefins **2** has been realized[2] in the presence of naphthalene-diimides (NDIs).[10,12] Their π-acidic surface has been introduced as ideal for differentiating between planar MHT tautomers with delocalized charges (as in reactive intermediate **RI1**, Figure 1 d) and deplanarized tautomers with charges localized on the carboxylate (as in **RI2**). This discrimination was expected to influence the energy of the transition states leading to enolate addition and decarboxylation in different ways and thus to control the selectivity of the reaction. However, in our original design, the catalytic amine was positioned quite far from the π surface. Ion pairing to the conjugate ammonium cation should also remove the MHT anion from this surface (**RI3**, Figure 1 b), enabling the nitro-olefin acceptor **2** on the π surface to be approached by the MHT from above or in a "top-down" fashion (transition state **TS1**, Figure 1 c). This architecture should thus provide excellent stabilization of nitronate intermediates by anion–π interactions while having minimal influence on the equilibrium between the MHT tautomers, which results in poor selectivity. The objective of the present study was to develop general design strategies to enhance selectivity by 1) moving the MHT substrates as close as possible to the π surface (Figure 1 d), that is, to have the enolate approach the nitro-olefin from below or in a "bottom-up" fashion, and by 2) allowing the nitronate to reach the π surface only upon its formation during enolate addition (**TS2**, Figure 1 e). The significance of the results described herein suggests that the newly introduced, rigidified Leonard turns[13] represent a gen-

eral design principle for enabling reactions to occur on aromatic surfaces and thus for harnessing the full potential of anion–π,[2,5–8,10,11] cation–π,[4] and ion pair–π interactions[9] for catalysis.

The new catalysts and controls **5–19** were designed and synthesized based on lessons learned from the original catalysts **20–24** (Figure 2; for details on their synthesis and evaluation under standard conditions, see the Supporting Information). Anion–π catalyst **9** was conceived as the starting point for our systematic study. Kept as simple as possible, it contains a single NDI surface with two ethylsulfide substituents as handles to tune the π acidity (R^1),[14] an L-leucyl-*n*-hexylamide tail to ensure solubility (R^2), and a Leonard turn in its purest form.

Introduced almost fifty years ago[13] as trimethylene chains, Leonard turns can be considered more generally as three tetrahedral atoms that are in a half-chair conformation and attached to an aromatic surface at one end. The first atom following at the other end will find itself at a very short distance from the aromatic system, literally forced to be on top of the *ipso* atom of the aromatic ring. Leonard turns have been used extensively in functional systems, often not explicitly.[6,9,11,15] In catalyst **9**, the Leonard turn consists of two methylene groups and the sp³-hybridized nitrogen atom of the amine base.[6] The proton transferred to this nitrogen atom should then end up at a short distance above the imide nitrogen atom of the NDI, which in turn should place the MHT carbonyl group at the positive end of the imide carbonyl
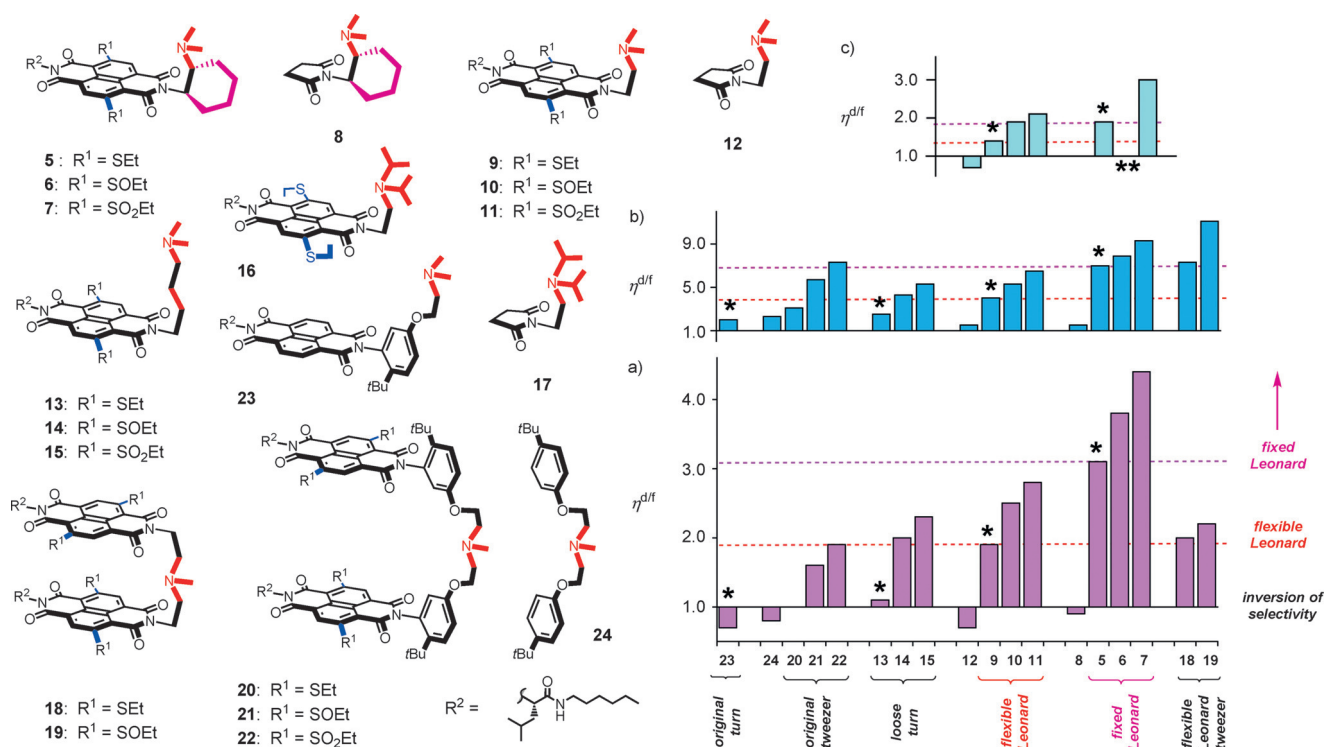

Figure 2. a) Catalyst selectivity, $\eta^{d/f} = \eta^d/\eta^f$, that is, the yield η^d of the intrinsically disfavored product (**3a**) divided by the yield η^f of the favored product (**4a**) in the presence of catalysts **5–24** in [D₈]THF at 20°C. b) Catalyst selectivity at 7°C for **3a** and **4a**. c) Catalyst selectivity at 7°C for **3b** and **4b**. All sulfoxides were isolated as mixtures of stereoisomers. See Table 1 for exact values and conditions. * Most important trends with comparable structures. ** Not measured.

moieties, in line with the bonds leading to the naphthalene (Figures 1 d, e).

In view of these considerations, we were delighted to find that under routine conditions at 20°C,[2] our first Leonard catalyst **9** catalyzed the addition of MAHT **1a** to nitroolefin **2** selectively: The intrinsically disfavored (d) addition product **3a** was obtained in $\eta^d = 65\%$ yield, with the naturally more favored (f) decarboxylation product **4a** generated in $\eta^f = 34\%$ (Table 1, entry 5). The resulting selectivity, $\eta^{d/f} = 1.9$, was outstanding considering that the original catalyst **23**, which features a loose turn, failed to cause the desired selectivity inversion ($\eta^{d/f} = 0.8$; Figure 2a and Table 1, entry 19). The new Leonard catalyst **9**, as simple as it gets, was already as good as the most developed original tweezer catalyst **22**, with two NDIs next to the amine and two sulfones in the NDI core maximizing effective molarity and π acidity, respectively (Figure 2a and Table 1, entry 18). Increasing selectivity upon oxidation of the sulfides in the core of **9** to sulfoxides in **10** and sulfones in **11** ($\eta^{d/f} = 2.5$ and 2.8) and the absence of selectivity inversion with control catalyst **12** without a π surface ($\eta^{d/f} = 0.7$) confirmed operational anion–π interactions in the presence of Leonard turns (Figure 2a and Table 1, entries 5–8).

Control compound **13**, with a loose tetramethylene turn, failed to perform as well as Leonard catalyst **9** (Figure 2a). However, increasing selectivity inversion with increasing π acidity in **13**–**15** revealed the existence of "tortoise-and-hare" anion–π catalysis also with looser turns (Table 1, entries 9–11). Control compound **16**, with a bulky Hünig's base analogue in the Leonard turn, performed only slightly better than control **17** without a π surface ($\eta^{d/f} = 0.9$ vs. $\eta^{d/f} = 0.7$; Table 1, entry 12 and 13), presumably because the steric crowding hinders operational anion–π interactions. Increasing the effective molarity of the π surfaces in tweezer-like Leonard catalysts **18** and **19** did not improve the outstanding activity of the most simple, most compact monomeric Leonard catalysts **9**–**11** (Figure 2a and Table 1, entries 14 and 15 vs. 5–7).

In catalyst **5**, the flexible Leonard turn of catalyst **9** is rigidified (see **TS2** in Figure 1e). In doing so, the selectivity inversion increased to $\eta^{d/f} = 3.1$ (Table 1, entry 1). Increasing the π acidity in catalysts **6** and **7** further improved the activity to $\eta^{d/f} = 3.8$ and $\eta^{d/f} = 4.4$ (Table 1, entries 2 and 3). The $\eta^{d/f} = 0.9$ value for control **8** without a π surface confirmed that these quite spectacular results originate from maximizing the anion–π interactions with the rigidified Leonard turn in catalysts **5**–**7**. Comparisons over the full series of comparable architectures, from original and loose turns in **23** ($\eta^{d/f} = 0.8$) and **13** ($\eta^{d/f} = 1.1$) to flexible Leonard turns in **9** ($\eta^{d/f} = 1.9$), beautifully illustrate the unique power of fixed Leonard turns in **5** ($\eta^{d/f} = 3.1$) to run reactions on π surfaces and maximize contributions from anion–π interactions for catalysis (Figure 2a). The same trend holds true at maximal π acidity, moving from $\eta^{d/f} = 2.3$ for loose turns in **15** to $\eta^{d/f} = 2.8$ with flexible Leonard turns in **9** and $\eta^{d/f} = 4.4$ with fixed Leonard turns in **7**.

Reactions run at 7°C instead of 20°C gave the same overall trends (Figure 2b). For example, the steady increase from original and loose turns in **23** ($\eta^{d/f} = 2.3$) and **13** ($\eta^{d/f} = 2.5$) to flexible Leonard turns in **9** ($\eta^{d/f} = 4.1$) and fixed Leonard turns in **5** ($\eta^{d/f} = 7.0$) remained intact (Figure 2a). The overall higher selectivity is consistent with the notion of strengthened anion–π interactions at lower temperatures. In this instance, the impact of flexible as well as fixed Leonard turns was less pronounced, whereas the effective molarity of the π surfaces became more important. For example, loose tweezers **22** at maximal π acidity reached the selectivity of fixed Leonard turns **5** at minimal π acidity (Figure 2b); at 20°C, **22** was clearly less active than **5** (Figure 2a). Moreover, the overall best performance was found for tweezers **19** with flexible Leonard turns and intermediate π acidity ($\eta^{d/f} = 11.1$), although the fixed Leonard turns in monomeric **7** were almost as good ($\eta^{d/f} = 9.3$, Figure 2b); at 20°C, **19** was much less selective than **7** and also **5** (Figure 2a). This overall reduced importance at lower temperature

Table 1: Characteristics of the anion–π catalysts and control compounds.[a]

	Cat.[b]	π Acidity[c]	Substrate[d]	η^d [%][e]	η^f [%][f]	$\eta^{d/f}$[g]	$\Delta\Delta G_{TS}^{\ddagger}$ [kJ mol^{-1}][h]
1	**5**	+	**1a**	84 (74)	12 (24)	7.0 (3.1)	−3.6 (−3.0)
2	**6**	++	**1a**	87 (77)	11 (20)	7.9 (3.8)	−3.9 (−3.5)
3	**7**	+++	**1a**	86 (80)	9 (18)	9.6 (4.4)	−4.3 (−3.9)
4	**8**	−	**1a**	57 (47)	39 (52)	1.5 (0.9)	−
5	**9**	+	**1a**	78 (65)	19 (34)	4.1 (1.9)	−2.3 (−2.3)
6	**10**	++	**1a**	80 (68)	15 (27)	5.3 (2.5)	−2.9 (−2.9)
7	**11**	+++	**1a**	84 (74)	13 (26)	6.5 (2.8)	−3.4 (−3.4)
8	**12**	−	**1a**	59 (43)	40 (56)	1.5 (0.7)	−
9	**13**	+	**1a**	70 (50)	28 (47)	2.5 (1.1)	−1.2 (−1.1)
10	**14**	++	**1a**	81 (64)	19 (32)	4.3 (2.0)	−2.4 (−2.6)
11	**15**	+++	**1a**	83 (68)	16 (30)	5.2 (2.3)	−2.9 (−2.9)
12	**16**	+	**1a**	73 (43)	25 (48)	2.9 (0.9)	−1.5 (−0.6)
13	**17**	−	**1a**	(40)	(54)	(0.7)	−
14	**18**	+	**1a**	87 (51)	12 (23)	7.3 (2.0)	−3.7 (−2.6)
15	**19**	++	**1a**	89 (54)	8 (27)	11.1 (2.2)	−4.6 (−3.4)
16	**20**	+	**1a**	71 (50)	23 (48)	3.1 (1.0)	−1.2 (−0.9)
17	**21**	++	**1a**	80 (59)	14 (36)	5.7 (1.6)	−2.9 (−2.0)
18	**22**	+++	**1a**	80 (59)	11 (31)	7.3 (1.9)	−3.5 (−2.6)
19	**23**	+	**1a**	69 (46)	30 (54)	2.3 (0.8)	−0.7 (−0.8)
20	**24**	−	**1a**	60 (37)	30 (53)	2.0 (0.7)	−
21	**5**	+	**1b**	65	34	1.9	−2.3
22	**7**	+++	**1b**	74	25	3.0	−3.4
23	**9**	+	**1b**	59	41	1.4	−1.6
24	**10**	++	**1b**	64	33	1.9	−2.3
25	**11**	+++	**1b**	68	32	2.1	−2.6
26	**12**	−	**1b**	42	57	0.7	−

[a] Reactions were conducted in [D$_8$]THF with 20 mol% of the catalyst and monitored by ^{1}H NMR spectroscopy. [b] Catalysts, see Figure 2 for their structures. [c] Qualitative indication of the π acidity, − = no π surface. [d] Substrates; **1a**: 200 mM with 2 M **2**; **1b**: 200 mM with 1.5 M **2**. [e] Yield of the intrinsically disfavored products **3a/3b** in THF at 7°C (in parentheses: η^d at 20°C). [f] Yield of the intrinsically favored products **4a/4b** at 7°C (20°C). [g] Selectivity $\eta^{d/f} = \eta^d/\eta^f$ at 7°C (20°C). [h] Selective catalysis: The difference in the Gibbs free energies $\Delta G_{TS}^{\ddagger}$ (catalyst) of the two transition states leading to the intrinsically favored (f) and disfavored (d) products, calibrated against the nearest control $\Delta G_{TS}^{\ddagger}$ (**8**, **12**, **17**, **24**); $\Delta G_{TS}^{\ddagger} = -RT\ln(\eta^{d/f})$,[16] $\Delta\Delta G_{TS}^{\ddagger} = \Delta G_{TS}^{\ddagger}$ (catalyst) − $\Delta G_{TS}^{\ddagger}$ (control). Data for **20**–**24** are from Ref. [2].

suggests that the contributions from flexible and in particular those from fixed Leonard turns are mainly entropic, that is, a most practical and most significant expression of the classical concept of preorganization.

It has been established previously[2] that a combination of selective deceleration of the intrinsic decarboxylation in favor of accelerating the disfavored addition gives rise to the observed inversion of selectivity. These most intriguing trends were expected to emerge from the ability of anion–π interactions to distinguish the planar MHT enolate as in **RI1** from the non-planar malonate tautomer as in **RI2** (Figure 1 d). Assuming a Curtin–Hammett situation where the two classes of tautomers are in rapid equilibrium, the difference in Gibbs free energy $\Delta G_{TS}^{\ddagger}$ of the two transition states leading to addition (d) or decarboxylation (f) is determined by the ratio d/f of the products (Table 1).[16] The resulting $\Delta G_{TS}^{\ddagger}$ values of the catalysts were then calibrated against the background contributions of amine bases without nearby π-acidic surfaces. The dependence of the obtained $\Delta\Delta G_{TS}^{\ddagger}$ values (Table 1) on the π acidity was roughly linear for fixed Leonard turns in **5–7** (♦), flexible Leonard turns in **9–11** (■), and loose turns in catalysts **13–15** (○; Figure 3). The

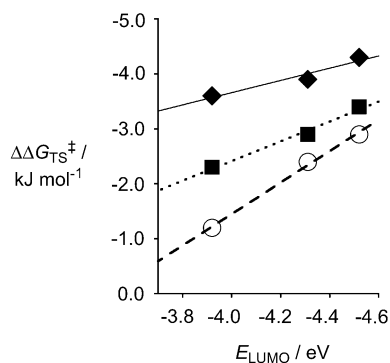***Figure 3.*** Differential transition-state stabilization $\Delta\Delta G_{TS}^{\ddagger}$ for **5–7** (♦, vs. **8**), **9–11** (■, vs. **12**), and **13–15** (○, vs. **12**) as a function of the LUMO energies for NDIs with sulfides (−3.92 eV), sulfoxides (−4.31 eV), and sulfones (−4.52 eV) in the core, at 7°C. Negative $\Delta\Delta G_{TS}^{\ddagger}$ values indicate selective acceleration of the disfavored over the favored reaction.

slopes, however, were clearly different. This difference, namely steeper slopes for less preorganized turns, provided corroborative experimental evidence that the significance of flexible and fixed Leonard turns, in particular, increases with decreasing π acidity. This finding is consistent with the increasing importance of Leonard turns with increasing temperature (Figure 2 a vs. 2 b). Therefore, it can be concluded that precisely engineered turns enable efficient anion–π catalysis to take place even with relatively weak π acidity. When the aromatic surface is strongly electron-deficient, anion–π catalysis takes place efficiently even when substrate placement (i.e., the constituent nature of the Leonard link) is less than ideal.

Having found a powerful method to position a substrate on a π-acidic surface, compatibility with substrates other than MHTs was tested with β-keto acids **1b** (Figure 1). These

substrates readily decarboxylate in solution.[17] However, with a suitable catalyst, they too are capable of adding to nitro-olefins.[18] Under standard reaction conditions at ambient temperature, it was found that β-keto acids decarboxylate more rapidly than MHTs. Consequently, all reactions were conducted at 7°C (see the Supporting Information). A rise in product selectivity with increasing π acidity of the catalysts, along with the confirmation of selectivity inversion with control **12** at low temperature ($\eta^{d/f} = 0.7$), are already strong indicators for operational anion–π interactions analogous to the results observed with MHT substrates. Indeed, the use of flexible Leonard turns increased the selectivity from $\eta^{d/f} = 1.4$ for sulfide **9** to $\eta^{d/f} = 1.9$ for sulfoxide **10** and $\eta^{d/f} = 2.1$ for sulfone **11** (Figure 2 c and Table 1, entries 23–25). As anticipated, fixed Leonard turns at minimal π acidity in **5** were as good as flexible turns at maximal π acidity in **11** (Table 1, entries 22 and 26). Indeed, fixed Leonard turns at maximal π acidity in **7** afforded a selectivity of $\eta^{d/f} = 3.0$—the highest selectivity—demonstrating that rigidifying a Leonard turn is equally applicable as a strategy for promoting the successful formation of intrinsically disfavored addition products with β-keto acids.

Compared to other noncovalent interactions, such as hydrogen, halogen, or chalcogen bonds, in catalysis,[19] interactions with aromatic surfaces are much less directional, thus creating the challenge to ideally place a substrate on such a π surface. This study offers a general and practical solution. Currently, we are most interested in applying the lessons learned to other reactions[20] and to more complex systems.[21,22]

[1] J. Staunton, K. J. Weissman, *Nat. Prod. Rep.* **2001**, *18*, 380–416.
[2] Y. Zhao, S. Benz, N. Sakai, S. Matile, *Chem. Sci.* **2015**, *6*, 6219–6223.
[3] a) J. Lubkoll, H. Wennemers, *Angew. Chem. Int. Ed.* **2007**, *46*, 6841–6844; *Angew. Chem.* **2007**, *119*, 6965–6968; b) Y. Pan, C. W. Kee, Z. Jiang, T. Ma, Y. Zhao, Y. Yang, H. Xue, C. H. Tan, *Chem. Eur. J.* **2011**, *17*, 8363–8370.
[4] a) D. A. Stauffer, R. E. Barrans, Jr., D. A. Dougherty, *Angew. Chem. Int. Ed. Engl.* **1990**, *29*, 915–918; *Angew. Chem.* **1990**, *102*, 953–956; b) R. R. Knowles, S. Lin, E. N. Jacobsen, *J. Am.*

4278 www.angewandte.org

© 2016 Wiley-VCH Verlag GmbH & Co. KGaA, Weinheim

Angew. Chem. Int. Ed. **2016**, *55*, 4275–4279

Chem. Soc. **2010**, *132*, 5030 – 5032; c) Q. Zhang, K. Tiefenbacher, *Nat. Chem.* **2015**, *7*, 197 – 202.

[5] a) M. Giese, M. Albrecht, K. Rissanen, *Chem. Rev.* **2015**, *115*, 8867 – 8895; b) H. T. Chifotides, K. R. Dunbar, *Acc. Chem. Res.* **2013**, *46*, 894 – 906; c) A. Frontera, P. Gamez, M. Mascal, T. J. Mooibroek, J. Reedijk, *Angew. Chem. Int. Ed.* **2011**, *50*, 9564 – 9583; *Angew. Chem.* **2011**, *123*, 9736 – 9756; d) D.-X. Wang, M.-X. Wang, *Chimia* **2011**, *65*, 939 – 943; e) P. Ballester, *Acc. Chem. Res.* **2013**, *46*, 874 – 884.

[6] a) A. Frontera, F. Saczewski, M. Gdaniec, E. Dziemidowicz-Borys, A. Kurland, P. M. Deyà, D. Quiñonero, C. Garau, *Chem. Eur. J.* **2005**, *11*, 6560 – 6567; b) M. Giese, M. Albrecht, K. Wiemer, A. Valkonen, K. Rissanen, *New J. Chem.* **2012**, *36*, 1368 – 1372; c) M. Giese, M. Albrecht, K. Rissanen, *Chem. Commun.* **2016**, *52*, 1778 – 1795.

[7] a) Q. He, Y.-F. Ao, Z.-T. Huang, D.-X. Wang, *Angew. Chem. Int. Ed.* **2015**, *54*, 11785 – 11790; *Angew. Chem.* **2015**, *127*, 11951 – 11956; b) S. T. Schneebeli, M. Frasconi, Z. Liu, Y. Wu, D. M. Gardner, N. L. Strutt, C. Cheng, R. Carmieli, M. R. Wasielewski, J. F. Stoddart, *Angew. Chem. Int. Ed.* **2013**, *52*, 13100 – 13104; *Angew. Chem.* **2013**, *125*, 13338 – 13342.

[8] A. Vargas Jentzsch, S. Matile, *J. Am. Chem. Soc.* **2013**, *135*, 5302 – 5303.

[9] K. Fujisawa, M. Humbert-Droz, R. Letrun, E. Vauthey, T. A. Wesolowski, N. Sakai, S. Matile, *J. Am. Chem. Soc.* **2015**, *137*, 11047 – 11056.

[10] a) Y. Zhao, Y. Domoto, E. Orentas, C. Beuchat, D. Emery, J. Mareda, N. Sakai, S. Matile, *Angew. Chem. Int. Ed.* **2013**, *52*, 9940 – 9943; *Angew. Chem.* **2013**, *125*, 10124 – 10127; b) A. Berkessel, S. Das, D. Pekel, J.-M. Neudörfl, *Angew. Chem. Int. Ed.* **2014**, *53*, 11660 – 11664; *Angew. Chem.* **2014**, *126*, 11846 – 11850; c) Y. Zhao, Y. Cotelle, A.-J. Avestro, N. Sakai, S. Matile, *J. Am. Chem. Soc.* **2015**, *137*, 11582 – 11585; d) K. S. Lee, J. R. Parquette, *Chem. Commun.* **2015**, *51*, 15653 – 15656; e) F. N. Miros, Y. Zhao, G. Sargsyan, M. Pupier, C. Besnard, C. Beuchat, J. Mareda, N. Sakai, S. Matile, *Chem. Eur. J.* **2016**, *22*, 2648 – 2657.

[11] Y. Zhao, C. Beuchat, Y. Domoto, J. Gajewy, A. Wilson, J. Mareda, N. Sakai, S. Matile, *J. Am. Chem. Soc.* **2014**, *136*, 2101 – 2111.

[12] a) S.-L. Suraru, F. Würthner, *Angew. Chem. Int. Ed.* **2014**, *53*, 7428 – 7448; *Angew. Chem.* **2014**, *126*, 7558 – 7578; b) S. V. Bhosale, C. H. Jani, S. J. Langford, *Chem. Soc. Rev.* **2008**, *37*, 331 – 342.

[13] N. J. Leonard, *Acc. Chem. Res.* **1979**, *12*, 423 – 429.

[14] J. Míšek, A. Vargas Jentzsch, S. I. Sakurai, D. Emery, J. Mareda, S. Matile, *Angew. Chem. Int. Ed.* **2010**, *49*, 7680 – 7683; *Angew. Chem.* **2010**, *122*, 7846 – 7849.

[15] a) I. Richter, J. Minari, P. Axe, J. P. Lowe, T. D. James, K. Sakurai, S. D. Bull, J. S. Fossey, *Chem. Commun.* **2008**, 1082 – 1084; b) K. Avasthi, A. Ansari, A. K. Tewari, R. Kant, P. R. Maulik, *Org. Lett.* **2009**, *11*, 5290 – 5293.

[16] J. I. Seeman, *Chem. Rev.* **1983**, *83*, 83 – 134.

[17] F. Zhong, W. Yao, X. Dou, Y. Lu, *Org. Lett.* **2012**, *14*, 4018 – 4021.

[18] H. W. Moon, D. Y. Kim, *Tetrahedron Lett.* **2012**, *53*, 6569 – 6572.

[19] a) S. H. Jungbauer, S. M. Huber, *J. Am. Chem. Soc.* **2015**, *137*, 12110 – 12120; b) A. Bauzá, T. J. Mooibroek, A. Frontera, *ChemPhysChem* **2015**, *16*, 2496 – 2517.

[20] Promising preliminary results with other reactions will be reported in due course.

[21] B. Baumeister, N. Sakai, S. Matile, *Org. Lett.* **2001**, *3*, 4229 – 4232.

[22] All chiral anion–π catalysts tested performed with negligible enantioselectivity, independent of the solvent and temperature (< 7 % *ee*, not shown). However, preliminary results show that when integrated into complex systems, catalyst **5** can afford **3a** in up to 95 % *ee*.